EVALUATION OF COMPRESSION TESTING METHODS FOR THE CORTICAL RING IN THE DISTAL FEMUR METAPHYSIS OF ADULT MALE RATS

An Honors Fellow Thesis

by

RYAN SPENCER BISHOP

Submitted to Honors and Undergraduate Research
Texas A&M University
in partial fulfillment of the requirements for the designation as

HONORS UNDERGRADUATE RESEARCH FELLOW

May 2012

Major: Mechanical Engineering

EVALUATION OF COMPRESSION TESTING METHODS FOR THE CORTICAL RING IN THE DISTAL FEMUR METAPHYSIS OF ADULT MALE RATS

An Honors Fellow Thesis

by

RYAN SPENCER BISHOP

Submitted to Honors and Undergraduate Research
Texas A&M University
in partial fulfillment of the requirements for the designation as

HONORS UNDERGRADUATE RESEARCH FELLOW

Approved by:

Research Advisor: Harry Hogan
Associate Director, Honors and Undergraduate Research: Duncan MacKenzie

May 2012

Major: Mechanical Engineering

ABSTRACT

Evaluation of Compression Testing Methods for the Cortical Ring in the Distal Femur Metaphysis of Adult Male Rats. (May 2012)

Ryan Spencer Bishop
Department of Mechanical Engineering
Texas A&M University

Research Advisor: Dr. Harry Hogan
Department of Mechanical Engineering

The characterization of bone loss in astronauts continues to be a pressing health concern for astronauts who spend months aboard the International Space Station (ISS). Through the use of the hindlimb unloaded rat model, Hogan et. al. have compared the effect of unloading at different anatomical bone sites and compartments within the hindlimb bones. Because femur metaphysis bone specimens remain from a previous experiment that tested the cancellous compartment, the untested cortical rings remain to be characterized. However, due to the complex geometry and composition of the cortical bone, an appropriate testing method must be identified which will effectively evaluate the effect of hindlimb unloading on this bone tissue. This study compared the use of axial and diametral compression testing in evaluating the intrinsic properties, namely, ultimate stress and elastic modulus, of the cortical ring of the femur metaphysis. In order to preserve the cortical specimens from the hindlimb unloaded study, practice bones (taken from rats not used or removed from the study) were tested. After approximating

the cortical geometry of each specimen, the bones were divided into axial and diametral compression testing groups (n=3), and the bones were compressed to failure.

Diametral testing was found to result in a much more consistent location of failure than the axial testing, but the standard deviations for the calculated ultimate stress and elastic modulus were considerably higher. Both the diametral and axial testing yielded properties that deviated significantly from those previously calculated for femoral diaphysis samples. This deviation is unsurprising, as the lack of recorded background and the dimensional approximations used to analyze the bones likely introduced errors that compromised accurate determination of absolute values. However, the results remain useful for comparison purposes. With more accurate measurement of cortical geometry and the use of the more consistently cut metaphysis samples from known testing conditions, both testing methods may yield properties closer to those found for the femoral diaphysis. Although the axial compression testing displayed more variation in the location of failure, this method is currently recommended because the calculated ultimate stress and elastic modulus values displayed significantly reduced variance.

DEDICATION

I would like to dedicate this thesis to my family for their support and prayers throughout the planning and execution of my research.

ACKNOWLEDGMENTS

I am indebted to Dr. Harry Hogan, Yasamin Shirazi, Ramon Boudreaux, and Estela Gonzalez for their indispensable assistance in the formulation and implementation of this thesis.

NOMENCLATURE

ISS	International Space Station
RPC	Reduced Platen Compression
BL	Baseline
AC	Aging Control
HU	Hindlimb Unloaded
pQCT	Peripheral Quantitative Computed Tomography

TABLE OF CONTENTS

Page

LIST OF FIGURES

CHAPTER I

INTRODUCTION

Motivation

Bone loss in astronauts who undergo skeletal unloading during extended spaceflight has been shown to be a significant health problem. Compared to losses of less than 1% per year in post-menopausal women, astronaut losses of 1-2% in the bone mineral density (BMD) from the femoral neck each month indicate a serious risk of bone fracture.[1, 2] Even more, studies conducted by Lang et al. found that ISS astronauts who had been in space 4.5-6 months displayed an incomplete recovery of bone mineral density and estimated bone strength, even one year later.[3] The safety of repeated trips to space is of particular importance as NASA may be forced to reduce the size of their astronaut corps to cut costs, thus increasing the number of astronauts making multiple missions.

There are numerous advantages to conducting animal studies in place of human experiments. One major advantage is that they are much more affordable than additional trips to space and even human bed rest studies. A second advantage is that animal bones can be excised and mechanically tested, an option which is not available in human studies. Because the hindlimb unloaded rat model has been well established as a ground-

---

This thesis follows the style of the *Journal of Bone and Mineral Research*.

based analog for simulating the effects of spaceflight on the musculoskeletal system, Dr. Harry Hogan has been using the model to address questions related to the effects on mechanical properties at various bone locations, namely: the midshaft of the femur and tibia, the femoral neck, and the cancellous bone in the distal femur metaphysis.[4] Although Bloomfield et. al. have found bone loss in microgravity simulations with hindlimb unloaded rats to display compartment-specific changes (cancellous vs. cortical regions of bone), the full extent of site-specific bone change is not yet fully understood.[5] Thus, questions still remain as to how the microgravity simulations affect variation in bone properties along different longitudinal locations of the bone as well as within the different types of bone tissue.

Previous experiments within this larger study have already conducted tests on bone samples obtained from hindlimb unloaded rats, and as a result there remain bone samples that are available for possible further testing. In particular, slices from the femur metaphysis remain after being subjected to RPC (reduced platen compression) testing of the cancellous bone.[6] This leaves the surrounding cortical ring to be analyzed. However, the more pressing question is how to test these remaining samples in such a way as to best identify the effects of hindlimb unloading on the cortical ring.

Objective

The primary purpose of this study is to evaluate the differences between axial and diametral compression testing on the mechanical properties of the cortical ring of the

distal femur metaphysis in adult male rats. This is to be accomplished by meeting the following objective:

To estimate mechanical properties of cortical bone (namely, the ultimate stress and the elastic modulus) through the use of both axial and diametral compression testing on cortical ring specimens, and to evaluate the two testing methods in terms of relative pros and cons and relevant salient features. This information will be important in evaluating which method is most suitable for use in testing the femur metaphysis samples remaining from the hindlimb unloaded rat study. The diametral testing method is hypothesized to yield calculated cortical properties closest to other regions of the femur because it loads different regions of the cortical specimens in compression and tension.

CHAPTER II

BACKGROUND

Bone anatomy and physiology

Bone is dense connective tissue that makes up the skeletal system in the human body. Functioning both as the primary load-bearing organ and in protection of more delicate internal organs, bones have both high strength and stiffness relative to most other biological tissues. The strength of bone tissue is in part brought about by its chemical composition, a combination of organic and inorganic components. The inorganic matrix, called hydroxyapatite, is made up of crystals of calcium phosphate, calcium carbonate, and calcium hydroxide and forms 65% of the bone. The organic component makes up the rest of the bone tissue and consists of cells and an organic matrix called osteoid, a combination of ground substance (glycosaminoglycans and glycoproteins) and collagen fibers (90% of organic component).[7] In the long bones of the body, bone tissue is typically divided into two compartments: cortical (also called compact) and cancellous (also called trabecular or spongy) (Fig. 1).

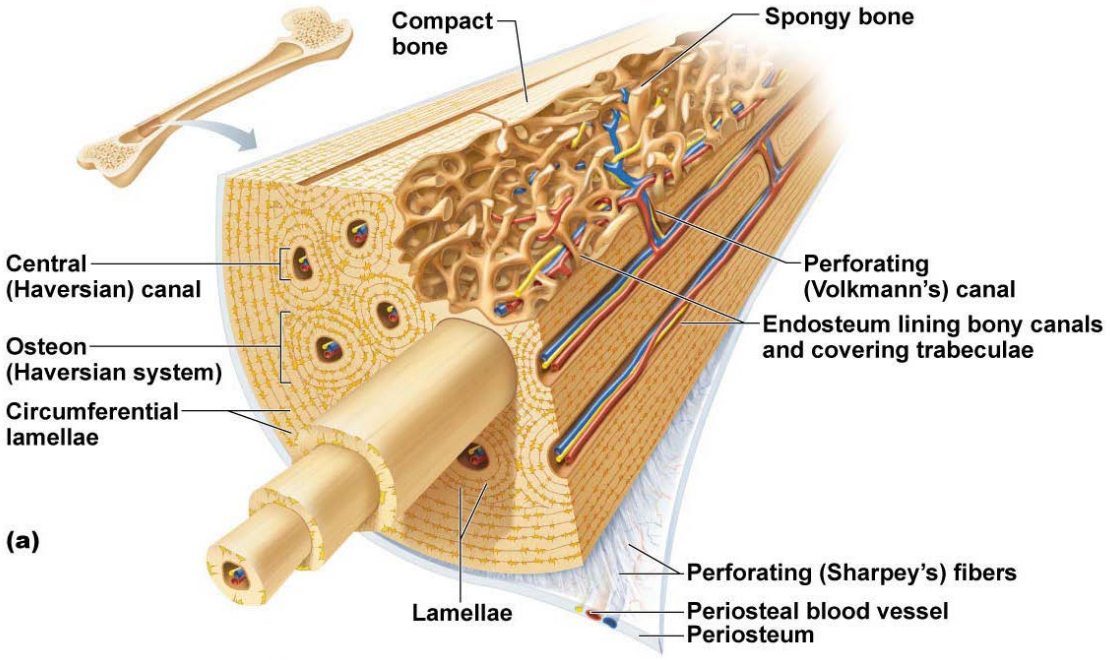

FIG. 1. Illustration of cortical and cancellous regions of bone.[8]

Cortical bone makes up the majority of the body's skeletal bone mass (80%) and bears the majority of the skeletal load due to its high stiffness relative to the cancellous bone. The basic structural unit of compact bone in humans is the osteon, a cylinder made up of concentric rings of bone matrix called lamellae. With collagen fibers oriented at different angles in each lamella and the stiff hydroxyapatite mineral, the osteon is able to resist both the compressive, tensile, bending, and torsional forces applied during bone use.[8] Cancellous bone forms a lattice of plates and rods (called trabeculae) that are aligned with force planes, and it provides a highly porous region for blood vessels and red marrow to vascularize the bone. Also called spongy or trabecular bone, cancellous bone is found primarily in the ends of long bones and the vertebrae.

The physiology of bone tissue is largely dependent on the activity of three types of bone cells: osteoblasts, osteoclasts and osteocytes. While osteoblasts and osteoclasts deposit new osteoid and resorb bone matrix, respectively, osteocytes are not completely understood, although they are thought to assist in the detection of microcracks and the triggering of osteoclast and osteoblast activity in bone remodeling.[7] While all three of these play an integral role during the modeling and initial growth involved in skeletal development, their activity applies to this study with regards to their role in the regulation of bone remodeling. In the context of this study, remodeling describes the process whereby osteoclasts and osteoblasts work simultaneously to remove and replace bone in order to maintain the load bearing capabilities of the bone. This dynamic and continuous process can have both negative and positive effects on bone strength. While the replacement of bone with microdamage and the adaptation of microstructure to bone stresses will benefit bone strength, the removal of trabeculae, the increase of cortical porosity, and the decrease of cortical thickness can decrease bone strength.[7] Because remodeling is dependent on mechanical usage, bone adapts to loading or disuse. Thus, bones change their mass and geometry in response to applied stresses.

The femur displays a structure typical to the long bones in the body with two ends called epiphyses, gradually tapering regions called metaphyses, and a central cortical shaft called a diaphysis. The distal femur metaphysis was chosen for evaluation because of its composite nature, including both cortical and cancellous regions. The different remodeling that occurs in cancellous and cortical bone due to disuse is an important part

of understanding astronaut femoral neck bone loss, which also has both cancellous and cortical regions.

Mechanical testing methods for rat distal femur metaphysis

Numerous mechanical tests can be used to evaluate the distal femur metaphysis. While micro- and nano-indentation techniques are commonly used to measure the mechanical properties of a single osteon or lamellae (respectively) of cortical bone, the strength of the bone microstructure or ultrastructure does not necessarily reveal the extrinsic (dependent on bone geometry and size) strength of a particular bone region. Tensile tests can be conducted on machined samples from femoral shaft, but this approach would likely not be effective in testing the thin cortical ring samples already obtained from the metaphysis. Compression testing was selected because it has been previously implemented in this larger bone study to test the cancellous region of test specimens obtained from the metaphysis.

Because the cancellous region responds more quickly than cortical to bone remodeling due to changes in mechanical loading (disuse or overload), it is often studied more extensively than cortical bone in bone studies.[7, 9] However, testing methods typically applied to the cancellous region can also be used to evaluate the cortical region. One example is the compression of a vertebra before and after removing the inner cancellous bone, a technique used to evaluate the vertebral cancellous region.[10] Whether the cancellous bone in the femur metaphysis is removed or not, axial compressive forces

exerted on the ring will almost entirely be loaded onto the cortical bone, as it is much stiffer than cancellous bone. Another method that has been more recently implemented is a diametral compression of cortical ring specimens obtained from the femoral neck.[11] The advantage of this method is that the bone is subjected to both axial and bending stresses, a loading that exerts tensile and compressive forces on the ring. Because crack propagation begins primarily due to tensile stresses, failure by compression typically occurs by deformation. Thus, the location of failure due to diametral compression should occur in the region of the cortical ring experiencing tension. This combined compressive and tensile loading is also informative to the astronaut study because it occurs during natural loading of the femoral neck (a high risk region for fracture) (Fig. 2).

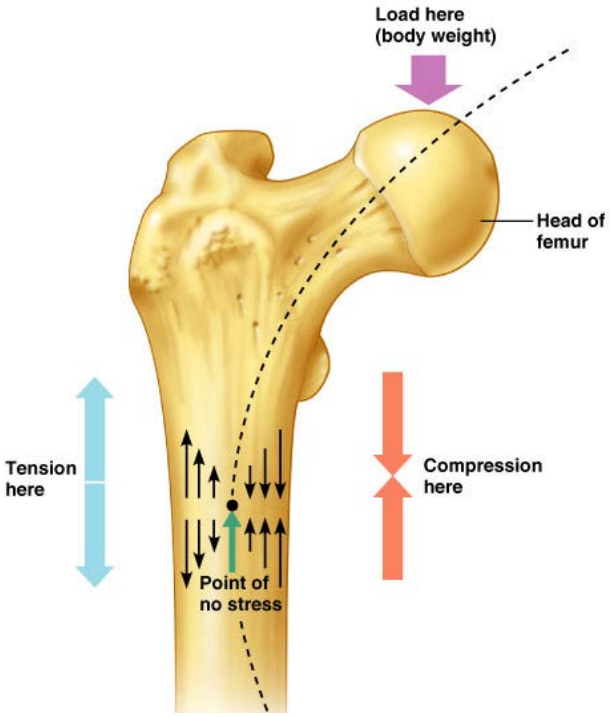

FIG. 2. Illustration of a loaded femoral neck specimen. The diagram shows how both compression and tension can be applied to a bone during natural usage.[8]

Both compression methods present significant advantages and complications due to the non-uniform cortical thickness and the slightly conical shape of the metaphyseal samples. Due to the tapering of the specimens, when loaded in axial compression, the cortical ring has the tendency to deflect radially outward as well causing hoop stresses to be experienced, instead of pure axial compression (Fig. 3). Despite this, the initial portion of the stress data obtained should be useful in determining the modulus. When loaded in diametral compression, the tapering of the cortical ring can cause only the largest diameter of the ring to initially contact the platen, resulting in unequal loading of the ring. Nevertheless, the combination of compressive and tensile forces exerted during the ring bending provides more interesting results as to the location and cause of failure. Thus, this experiment acted as a pilot study examining the feasibility of both methods before deciding which testing method should be used.

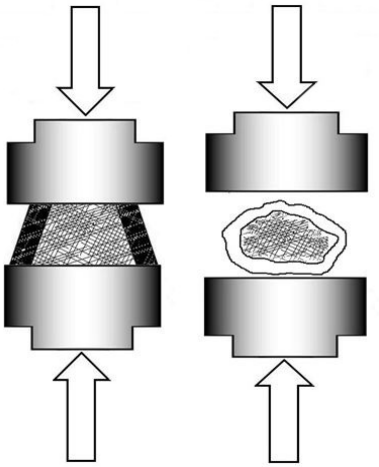

FIG. 3. Illustration of axial and diametral testing methods. On the left, a metaphyseal femur specimen (shown with cancellous interior and a cortical exterior shell) is loaded in axial compression. The tapering of the idealized specimen can be seen in that the ring

cross-section changes in the direction of compression. On the right, the ring is loaded in diametral compression. (Portion taken from Lemmon)[7]

Adult rat hindlimb unloading model

The broader goal of the study being conducted by the Texas A&M Department of Mechanical Engineering and the Department of Kinesiology is to evaluate how hindlimb unloading affects rat bone quality at various locations such that microgravity-induced bone loss experienced by astronauts can be better predicted after repeated missions to space. The hindlimb unloaded rat model was selected for this broader study due to its established usefulness in simulating microgravity induced skeletal bone loss.[4] The essential mechanism of the model is the use of a harness to raise the hindlimbs of adult rats, significantly reducing the loading of the hindlimb bones (Fig. 4).

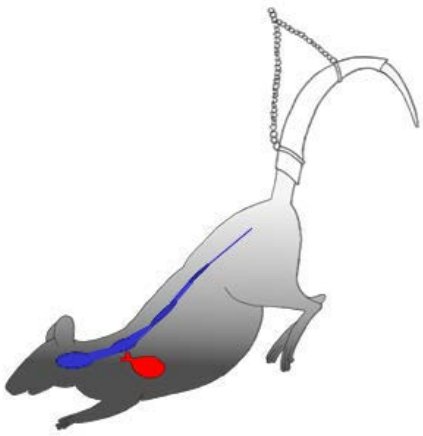

FIG. 4. Illustration of hindlimb unloaded rat. Subjected to disuse, a rat's hindlimbs undergo bone loss in a manner analogous to astronaut bone loss due to microgravity.[6]

The study began by obtaining male rats 6 months of age (considered skeletally mature age) and placing them into three general groups: an initial sacrifice group used to establish baseline bone measurements (BL), an aging control group (AC), and finally, a group designated to undergo hindlimb unloading (HU). Rats were hindlimb unloaded for twenty-eight day (1 month) periods of time (equivalent to astronaut bone loss) and were sacrificed at different times in order to observe any changes in the hindlimb bones.[5]

A parallel experiment to this discussed evaluation of metaphyseal cortical bone was conducted by cutting slices from the metaphysis of each rat and RPC testing the cancellous bone.[6] The remaining untested practice bone specimens (taken from rats removed or not used in the study) were tested in the current study. Although the condition of the practice bones was not recorded, the qualitative and quantitative results of compression testing can still be used to evaluate the general trends that will be observed in testing the cortical rings obtained from the rats.

CHAPTER III

METHODS

Specimen preparation and compression testing

The bone specimens from the femur metaphysis were previously cut using a 3242 Well Diamond Wire Saw. Because the samples were practice specimens, the cut thicknesses of the samples were not constant. In order to obtain approximate dimensions for the specimens, the cut thickness as well as the major and minor axes of each specimen was measured using a caliper, allowing cortical areas to be approximated as elliptical rings. The specimens were then separated into axial and diametral testing groups (n=3) by ordering the specimens from largest to smallest major axis, and then, alternating between groups while moving down the list. An Instron 3345 was used to perform the pilot tests for both axial and diametral compression to evaluate each method.

For both compression testing methods, two circular steel platens (with the upper platen having a 10 mm diameter) were attached with the bottom stationary and the top platen able to descend on the samples (Fig. 5). The specimens were placed such that each was completely underneath the upper platen. For the axial compression tests, each specimen was aligned with the larger diameter portion of the ring on the bottom. Because the samples were moistened using phosphate-buffered saline, no additional lubricant was needed on the platens to allow free movement. The upper platen was lowered until a pre-load of 0.01 N was observed and then the samples were compressed to failure. Force and

displacement were then recorded as the samples were compressed at a rate of 0.5 mm/min (within the limits of established compression testing) until a sharp decline in force was observed.[12]

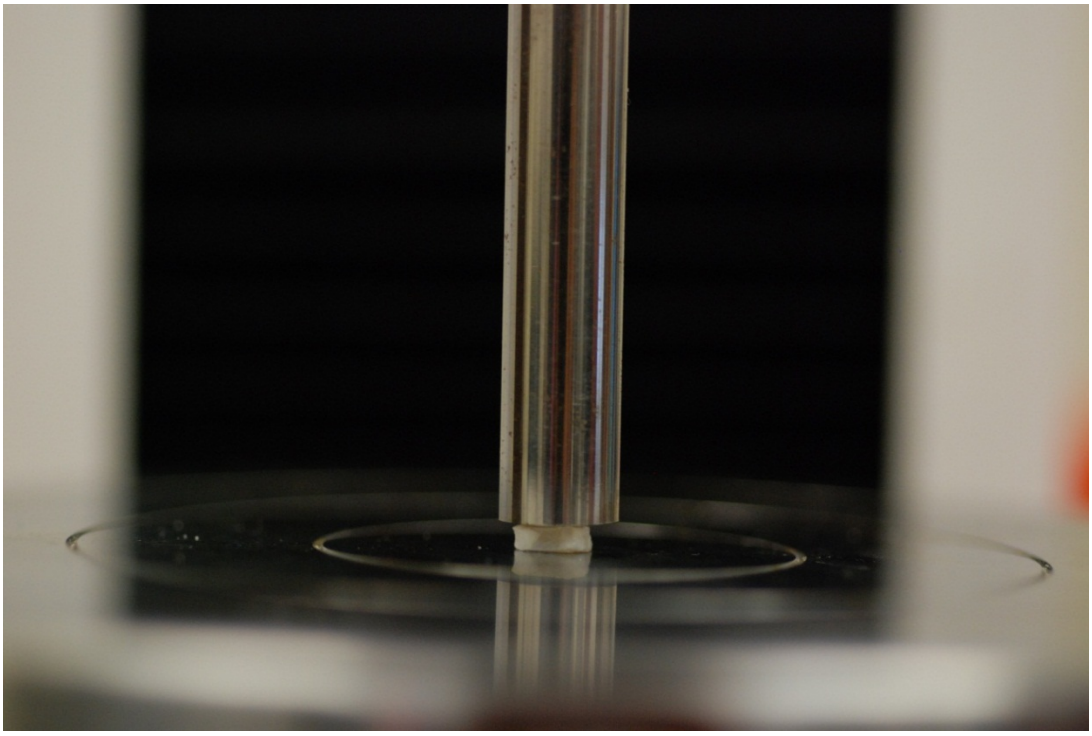

FIG. 5. Photograph of axial compression test with pre-loaded cortical specimen. As axial compression test is being performed, the upper platen descends and compresses the specimen to failure.

For the diametral compression test, again force and displacement were measured, but the samples were aligned with the cortical ring in the vertical plane and with the flatter end of the cortical ring functioning as a base (Fig. 6).

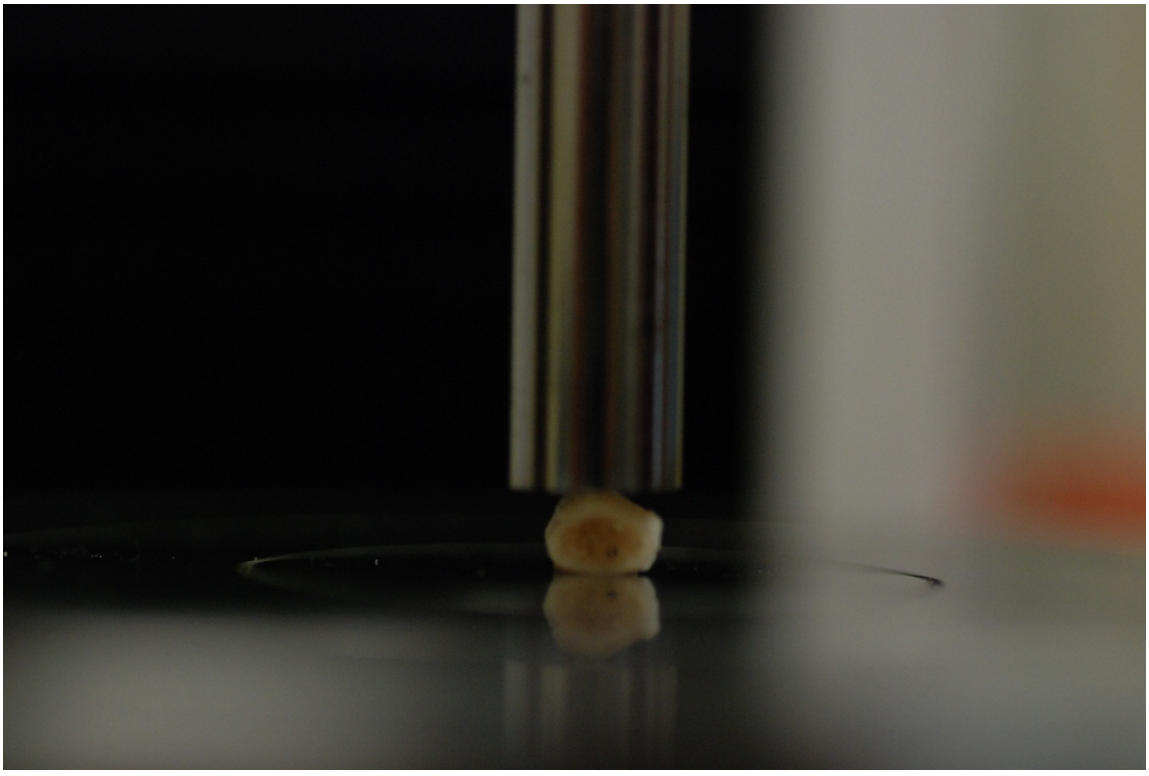

FIG. 6. Photograph of diametral compression test with pre-loaded cortical specimen.

Data reduction and analysis

The force and displacement data were exported into Excel from the Instron testing machine and analyzed using the following equations.

Axial compression

The force and displacement data (extrinsic or geometry-dependent quantities) were used to calculate what are called intrinsic properties, those which depend only on the material and not the geometry or structure. The following equations were used to calculate

ultimate stress (Eq. 1), strain (Eq. 2) and elastic modulus (Eq. 3) for the axially compressed specimens.

$$\sigma_u = \frac{F_{max}}{A_{cortical}} \quad (1)$$

$$\varepsilon = \frac{\Delta t}{t_0} \quad (2)$$

$$E = \frac{\sigma}{\varepsilon} = \frac{F_{max} t_0}{\Delta t A_{cortical}} = \frac{k t_0}{A_{cortical}} \quad (3)$$

Where $F_{max}$is the maximum measured force, $A_{cortical}$ is the cortical cross-sectional area under compression, t_0 is the original thickness of the specimen, Δt is the displacement, and k is the stiffness (taken here as the slope of the linear portion of the load displacement curve).

Diametral compression

Because, prior to the test, the diametral failure mode was unknown, stress equations were used to calculate the stresses at the four critical points on the ring. Analyzing the specimens as approximately circular rings, the equations for a curved beam were used to find the intrinsic properties (Fig. 7).

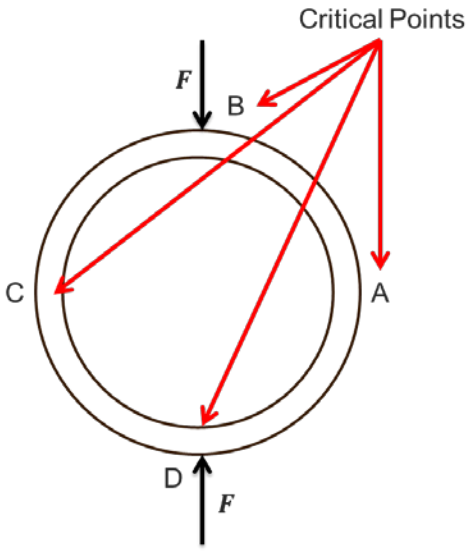

FIG. 7. Illustration of circular ring under diametral compressive loading by forces labeled *F*. The ends of the horizontal and vertical lines of symmetry for the ring undergo the largest compressive and tensile stresses during loading (labeled as points A, B, C, and D).

At points A and C, both bending and axial stresses are exerted on the ring. The axial force is compressive at all points through the ring radius. But, the bending moment causes the inner radius to experience compression and the outer radius to undergo tension. In contrast, points B and D experience no axial stress, but for bending the stresses are opposite, with the inner radius experiencing tensile stress and the outer radius undergoing compression. The radius of transition from tensile to compressive stress within the ring, known as the neutral axis, was calculated using the equation for a curved beam of rectangular cross-section. The radius to the centroid was approximated using the average between the measured major and minor axes of each bone specimen and the average cortical thickness for the baseline metaphysis bone samples included in

the study, calculated from pQCT (peripheral quantitative computed tomography) scans. (Eq. 4)

$$r_n = \frac{h}{\ln\left(\frac{r_o}{r_i}\right)} = \frac{h}{\ln\left(\frac{r_c + \frac{h}{2}}{r_c - \frac{h}{2}}\right)} \tag{4}$$

Where h is the average cortical thickness, r_o and r_i are the inner and outer radii of the ring, and r_c is the radius to the centroid.

Due to symmetry, only points A and B were analyzed. Castigliano's theorem was used to derive the moment experienced at points A and B. (Eq. 5 and 9) The axial and bending stresses were summed to calculate the total stress. (Eq. 6, 7, 8, and 10) In addition, using Castigliano's theorem to derive the deflection of the ring (Eq. 11), the elastic modulus was be calculated. (Eq. 12)

Point A

$$M_A = \frac{F_m R}{2}\left(1 - \frac{2}{\pi}\right) \tag{5}$$

$$\sigma_{bend}(r) = \frac{M\,(r - r_n)}{Aer} \tag{6}$$

$$\sigma_{axial} = \frac{0.5F_m}{A} \tag{7}$$

$$\sigma_A(r) = \sigma_{axial} + \sigma_{bend}(r) \tag{8}$$

Where F_m is the measured force, R is the approximated internal radius of the ring, r is the radius being evaluated, r_n is the neutral axis for a curved beam of rectangular cross-section, A is the cross-sectional area, and *e* is the eccentricity.

Point B

$$M_B = \frac{F_m R}{\pi} \tag{9}$$

$$\sigma_B = \sigma_{bend}(r) \tag{10}$$

$$\delta_B = \frac{\delta_m}{2} = \frac{F_m R^3}{4\pi EI}(\pi^2 - 8) \tag{11}$$

$$E = \frac{kR^3(\pi^2 - 8)}{2\pi I} \tag{12}$$

Where δ_m is the measured displacement, E is the elastic modulus, I is the second area moment of inertia for a rectangular beam, and k is the stiffness, approximated by taking slope of the linear region of the force versus displacement plot.

CHAPTER IV

RESULTS AND DISCUSSION

Observed failure modes

During the compression of each bone specimen, the bones were observed for any noticeable deformation or crack formation. The diametrally-loaded specimens showed clear deformation at points B and D, using the ring reference points established in Chapter III (Fig. 7). The compressive loads at the outer radius of these points resulted in indentations in the ring (Fig. 8).

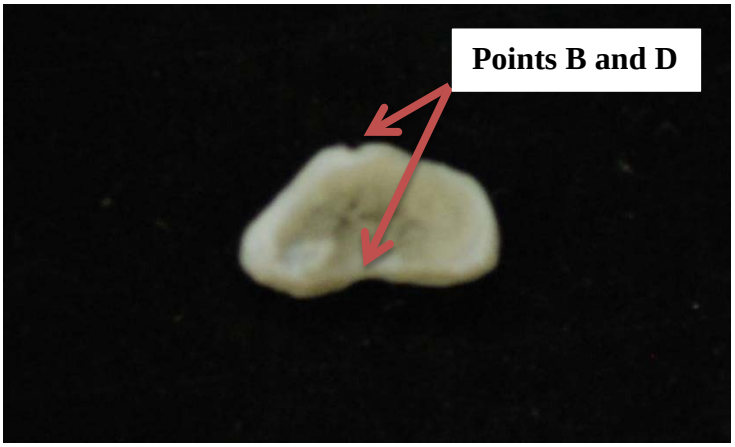

FIG. 8. A representative diametrally-loaded bone specimen after failure. Indentations were observed at ends of the minor axis (labeled points B and D from Chapter III).

The axially-loaded specimens did not show a consistent location of failure around the ring. But, the crack propagation was much more noticeable than in the diametrally-

loaded samples, as all axially loaded samples yielded cracks which passed completely through the cortical shell (Fig. 9).

FIG. 9. A representative axially-loaded bone specimen after failure.

Extrinsic cortical properties

Although the force and displacement data were expected to vary in magnitude between tests due to the different geometry of each sample and the tensile loading involved in the diametral compression, the trends observed for the axial and diametral tests remained consistent within each testing method. The diametral compression tests all displayed a pronounced rise in measured compressive force, followed by a gradual failure after the maximum force was reached (Fig. 10).

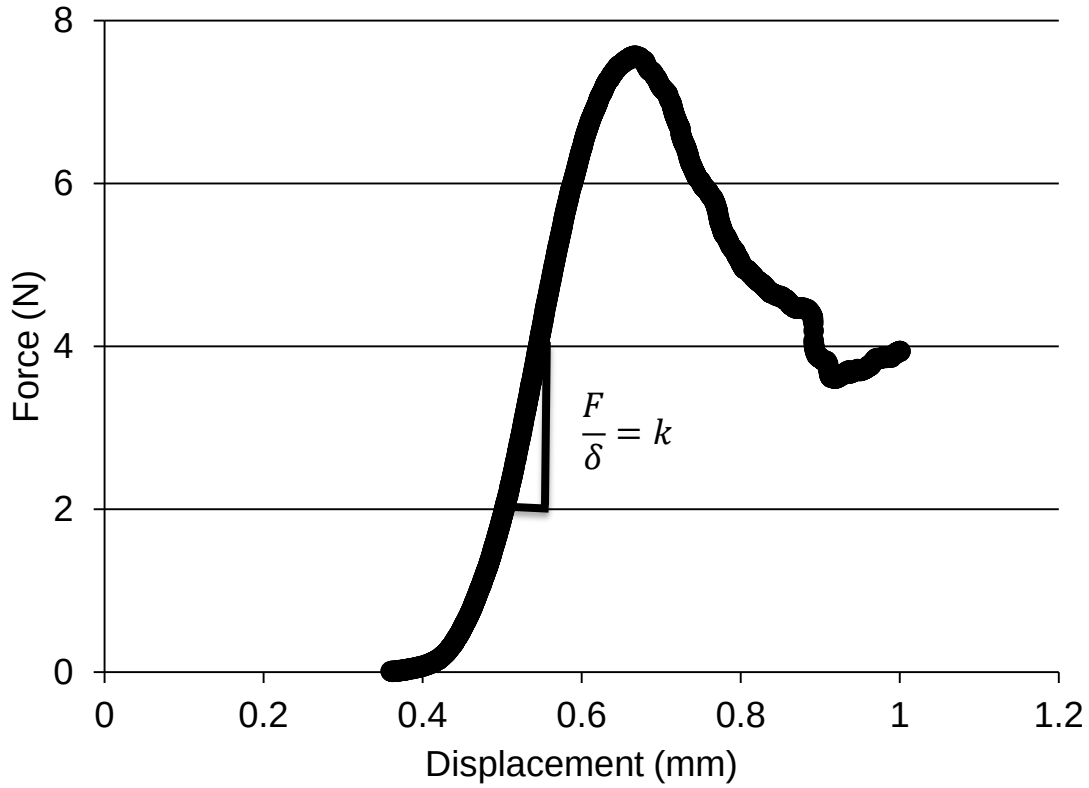

FIG. 10. A representative diametral compression force versus displacement plot. The stiffness value used to calculate elastic modulus was found by taking the slope of the linear region of the diametral compression force versus displacement curve.

In contrast, the axially-loaded samples all displayed a period of consolidation (for various lengths of time) during which the initially increasing measured force leveled off. Once the samples had consolidated to a degree, they continued to resist the compression with increasing force (in the second linear region), until they rapidly failed (Fig. 11).

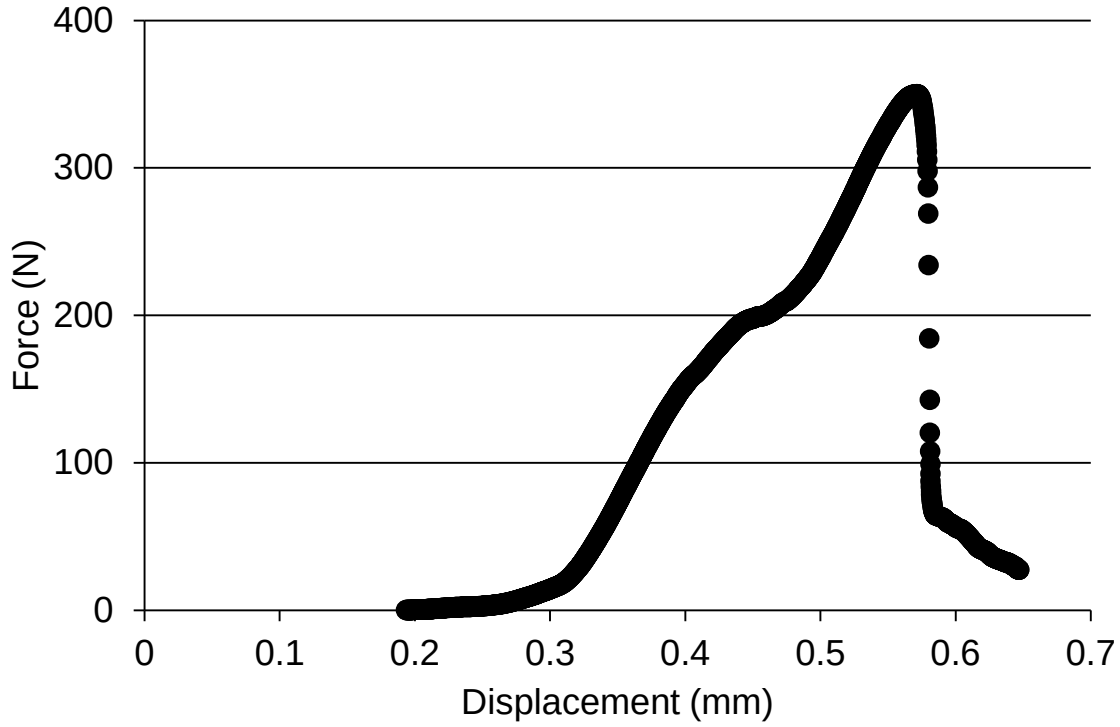

FIG. 11. A representative axial compression force versus displacement plot. The discussed consolidation period is observed at a displacement of ~0.45 mm. All the axially-loaded samples displayed rapid failure upon reaching their maximum compressive force.

Intrinsic cortical properties

In Table 1, a comparison of the calculated intrinsic properties for the practice bones to those of the femur in baseline rats revealed significant deviations in ultimate stress and elastic modulus.

Table 1. Average intrinsic properties for practice bones from femur metaphysis compared with values obtained by three-point bending of cortical bone in femur diaphysis specimens from baseline rats (not hindlimb unloaded).

	Ultimate Stress (MPa)	***Elastic Modulus (MPa)***
3-pt. Bending of Baseline Femur Diaphysis Specimens	132.49	4170
Diametral	45	5.1
Axial	20	0.2

This discrepancy could be contributed to several confounding factors. First, because the history of the tested practice bones was not recorded, the quality of the bones could be significantly diminished from that of the healthy baseline rats. Secondly, because ultimate stress and elastic modulus are dependent on the cortical area and the average cortical thickness, the approximation of the area as an elliptical ring and the use of the baseline metaphysis cortical thickness value for all of the samples tested may not have been close enough to the true area and thickness values. Finally, because the bones were not as precisely cut as later metaphysis specimens, the geometry of the practice bones may not have been as uniform. In particular, additional tapering of the ring through the ring thickness (cone-like geometry) could have caused both the diametral and the axial tests to load the bones in a manner which altered the failure.

Direct comparison of the two evaluated compression methods revealed that the diametral compression method calculated much higher values for both ultimate stress and elastic modulus (Fig. 12). Although its values were closer to those calculated for the femoral

diaphysis, the diametral compression samples displayed significantly higher standard deviations in both the average ultimate stress and elastic modulus values. This is likely because the location of failure was consistently under the loads, while the strength of the bone cross-sections under the loads may not have remained consistent between samples.

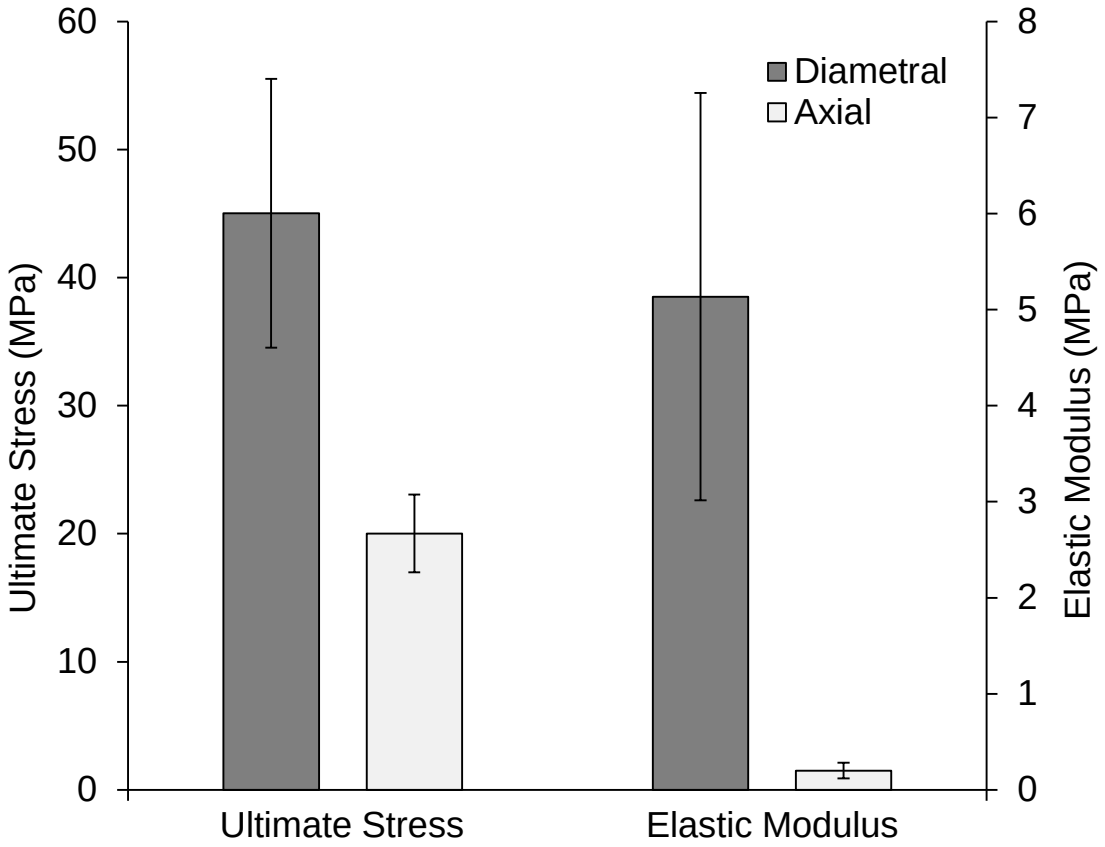

FIG. 12. Average ultimate stress and elastic modulus for the diametral and axial compression methods. Error bars represent standard deviation for the average of each calculated intrinsic property.

In contrast, the axial compression samples were not as constrained to fail at a single location on the ring. This likely led to the failure of the weakest link in the ring, at locations which may have been more comparable in strength.

CHAPTER V

CONCLUSIONS AND FUTURE DIRECTIONS

In contrast to the hypothesis offered in Chapter I, neither the diametral nor the axial compression of the metaphysis specimens yielded intrinsic properties which were close to those found for the femoral diaphysis. (Table 1) However, the small number of specimens tested using both methods (n=3) and the simplifying assumptions that were taken to analyze the practice bones available likely contributed to this incongruity. Experimental errors and artifacts could likely be reduced by more accurately measuring the cortical area used to calculate axial stress and the average cortical thickness used to calculate bending stress. Further, ensuring that all samples are cut to more consistent dimensions would improve accuracy as well. In addition, because the cortical specimens that remain to be tested were precisely cut to a nominal thickness of 2 mm starting at the intercondylar fossa of the femur, the amount of tapering in the specimens should be diminished and have less impact on the both compression methods.

Despite these imperfections, results from the current study are still useful and informative for gaining insight into the relative merits and characteristics of the two test methods and making initial comparisons. The location of failure for the diametral compression was much more consistent, as expected, because the test configuration dictates this to occur at sections under the load points (B and D in Fig. 7). Also, the values are closer in magnitude to the reference values from 3-point bending, and the load

vs. displacement curves are characterized by only a single monotonically increasing initial phase followed by the load peaking and declining steadily due to the progressive failure processes. However, variations in results were much higher for this method compared to axial compression, as reflected in the standard deviation error bars in Fig. 12. The main advantage of the axial compression test is that the results showed much less variability (smaller standard deviations). In closing, it should be emphasized and acknowledged that more definitive comparisons and well-justified recommendations will require larger sample sizes and more homogenous groups of specimens.

REFERENCES

1. Cauley JA, Lui LY, Stone KL, Hillier TA, Zmuda JM, Hochberg M, et al. 2005 Longitudinal study of changes in hip bone mineral density in Caucasian and African-American women. Journal of the American Geriatrics Society **53**:183-189.

2. Lang T, LeBlanc A, Evans H, Lu Y, Genant H, Yu A 2004 Cortical and trabecular bone mineral loss from the spine and hip in long-duration spaceflight. Journal of Bone and Mineral Research **19**:1006-1012.

3. Lang TF, Leblanc AD, Evans HJ, Lu Y 2006 Adaptation of the proximal femur to skeletal reloading after long-duration spaceflight. Journal of Bone and Mineral Research **21**:1224-1230.

4. Morey-Holton ER, Globus RK 1998 Hindlimb unloading of growing rats: A model for predicting skeletal changes during space flight. Bone **22**:83S-88S.

5. Bloomfield SA, Allen MR, Hogan HA, Delp MD 2002 Site- and compartment-specific changes in bone with hindlimb unloading in mature adult rats. Bone **31**:149-157.

6. Davis JM 2010 Characterization of the bone loss and recovery response at the distal femur metaphysis of the adult male hindlimb unloaded rat. M.S., Texas A&M University, College Station

7. Cowin SC, editor. 2001 Bone Mechanics Handbook. 2nd ed. Boca Raton, FL: CRC Press.

8. Hoehn ENMaK 2010 Human Anatomy and Physiology. 8th ed. San Francisco, CA: Pearson Benjamin Cummings.

9. Lemmon H 2003 Methods for reduced platen compression (RPC) test specimen cutting locations using micro-CT and planar radiographs. M.S., Texas A&M University, College Station

10. D. Chachra MLL, M. Kasra, M. D. Grynpas 2000 Differential effects of ovariectomy on the mechanical properties of cortical and cancellous bone in rat femora and vertebrae. Biomedical Sciences Instrumentation **2000**:123-128.

11. Devendra Bajaj RRBaJCF 2012 Evaluation of spatial variation in tissue-level mechanical properties of small animal cortical bone under diametral compression [Poster]. University of Medicine and Dentistry of New Jersey.

12. Hogan HA, Ruhmann SP, Sampson HW 2000 The mechanical properties of cancellous bone in the proximal tibia of ovariectomized rats. Journal of Bone and Mineral Research **15**:284-292.

CONTACT INFORMATION

Name:	Ryan Spencer Bishop
Professional Address:	c/o Dr. Harry Hogan Department of Mechanical Engineering MS 3123 Texas A&M University College Station, TX 77843
Email Address:	rsbishop1@gmail.com
Education:	B.S., Mechanical Engineering, Texas A&M University, December 2012 Undergraduate Research Fellow